Pluronic L64 Micelles near Cloud Point: Investigating the Role of Micellar Growth and Interaction in Critical Concentration Fluctuation and Percolation

ARTICLE *in* THE JOURNAL OF PHYSICAL CHEMISTRY B · JANUARY 2009

Impact Factor: 3.3 · DOI: 10.1021/jp808304w · Source: PubMed

4 AUTHORS, INCLUDING:

Rajib Ganguly
Bhabha Atomic Research Centre
61 PUBLICATIONS **918** CITATIONS
SEE PROFILE

Niharendu Choudhury
Bhabha Atomic Research Centre
57 PUBLICATIONS **1,060** CITATIONS
SEE PROFILE

Vinod K Aswal
Bhabha Atomic Research Centre
392 PUBLICATIONS **4,905** CITATIONS
SEE PROFILE

Pluronic L64 Micelles near Cloud Point: Investigating the Role of Micellar Growth and Interaction in Critical Concentration Fluctuation and Percolation

R. Ganguly,*,† N. Choudhury,‡ V. K. Aswal,§ and P. A. Hassan†

Chemistry Division, Theoretical Chemistry Section, and Solid State Physics Division, Bhabha Atomic Research Center, Mumbai 400 085, India

Received: September 18, 2008; Revised Manuscript Received: November 20, 2008

The structure and the properties of the (Ethylene Oxide)$_{13}$(Propylene Oxide)$_{30}$(Ethylene Oxide)$_{13}$ (Pluronic L64, MW $\approx$ 2900) micelles have been studied in the aqueous medium by small angle neutron scattering (SANS), dynamic light scattering (DLS) and viscometry measurements. The aqueous solutions of this triblock copolymer are unique among the pluronic solutions in showing critical concentration fluctuations and a concomitant enhancement in viscosity on approaching their cloud point. So far these results have been attributed solely to the presence of attractive interaction between the spherical L64 micelles. Recent theoretical studies, on the other hand, suggest that L64 micelles prefer a prolate ellipsoidal structure to sphere (Bedrov et al. *Langmuir* **2007**, *23*, 12032) and have a predominantly repulsive intermicellar interaction. A comparative analysis of our SANS data based on the spherical and prolate ellipsoidal structure shows that the L64 micelles can be best described by a prolate ellipsoidal structure, the aspect ratios of which increase progressively with increase in temperature. This, together with our viscosity and DLS studies, suggests that the enhanced viscosity of the copolymer solution near the cloud point arises largely due to the anisotropic growth of the micelles to the worm-like structures. The role of the intermicellar attractive interaction has thus been limited to the observed critical concentration fluctuation, and its effect decreases progressively with increase in copolymer concentration. It has also been shown that the water structure making salts like NaCl reduces the micellar growth temperature and helps in forming worm-like micelles at the room temperature. These studies thus identify the effect of micellar growth and interaction in determining the properties of the copolymer solution near the cloud point, which are the first of its kind in the case of the pluronics.

Introduction

Polyethylene oxide−polypropylene oxide−polyethylene oxide (PEO-PPO-PEO)-based triblock copolymers, known commercially as pluronics or poloxamers, are considered as an important class of nonionic surfactants because of their rich structural polymorphism and large range of applications.[1−12] These copolymers show a strong temperature dependence in their self-assembly characteristics in the aqueous medium, which arises due to the deteriorating solubility characteristics of their constituent blocks upon warming. Below their characteristic temperature, called the critical micellar temperature (CMT), both the PPO and the PEO blocks are soluble in water, and the copolymer molecules remain in the form of unimers. At the CMT the PPO blocks become insoluble and they form spherical micelles with PPO block as hydrophobic core and the hydrated PEO blocks as the corona.[7] At a temperature called the cloud point, the PEO blocks too become insoluble and the copolymers get phase-separated from water. Between CMT and the cloud point, a gradual increase in the hydrophobic character of the copolymer molecules with temperature leads to an increase in the aggregation number and the core size of their micelles. In the case of some of the copolymers, a sphere-to-rod micellar shape change is observed when the size of the core becomes equal to the length of the stretched hydrophobic chain.[13−16] For the pure copolymer solutions these sphere-to-rod shape transitions usually occur above 60 °C, and it can be brought down to room temperature or below by adding water-structure-making salts.[17−34] Such shape transitions are manifested in a large increase in the size of the copolymer micelles and a concomitant increase in the viscosity of the copolymer solutions. Although in the case of some of the copolymers such as P123, P85, P84, etc., such transitions are clearly identified, a similar set of manifestations shown by the aqueous L64 solutions have been explained based on intermicellar attractive interaction, mainly because of the observation of critical concentration fluctuation in them.[35−39] It has been suggested that the formation of large micellar clusters due to the presence of strong attractive interaction between the spherical L64 micelles leads to the observation of critical concentration fluctuation and the accompanying enhancement in the viscosity of the L64 solutions on approaching their cloud point. A recent theoretical paper based on implicit solvent molecular simulations,[40] however, suggests that the L64 micelles form only with prolate ellipsoidal structure and that the interaction between them is predominantly repulsive. The deviation from the spherical structure of the L64 micelles has been explained based on the minimization of their interaction energy at shorter separation due to the alignment of the micelles along the majority axis, and not by invoking the Israelachvili model,[41,42] which determines the micellar structures based on the hydrophobic chain length and hydrophilic headgroup area of the surfactant molecules. In view these diverse opinions about the structure and properties of the L64 micelles, we have carried out a systematic study on the structure and

* Corresponding author: E-mail: rajibg@barc.gov.in; Phone: +91- 22-25590286; Fax: + 9-22-25505151.
† Chemistry Division.
‡ Theoretical Chemistry Section.
§ Solid State Physics Division.

10.1021/jp808304w CCC: $40.75
Published on Web 12/29/2008

interaction of the L64 micelles in the aqueous medium as a function of temperature up to the cloud point. The studies throw light on the role of the micellar growth and the intermicellar interaction in the observations of critical concentration fluctuation and viscosity enhancement in the L64 solution on the verge of phase separation.

Materials and Methods

The triblock copolymer $EO_{13}PO_{30}EO_{13}$ (Pluronic L64) was procured from Aldrich. The copolymer solutions were prepared by weighing required amounts of solvents, copolymer, and salt (when needed) and keeping them in a refrigerator in tightly closed glass-stoppered vials for about one week. The absolute viscosities of the solutions at different temperatures were measured using calibrated Cannon Ubbelohde viscometers[43] in a temperature-controlled water bath. DLS measurements were carried out in the H_2O medium using a Malvern 4800 Autosizer with 7132 digital correlator. The light source was an argon ion laser operated at 514.5 nm with a maximum output power of 2 W. The average decay rate was obtained by analyzing the electric field autocorrelation function, $g^1(\tau)$, vs time data using a modified cumulants method as has recently been proposed.[44] This method overcomes the limitations of cumulants analysis to fit the data at long correlation time or large polydispersity.[45,46] For generating the average decay rate (Γ) vs q^2 plots (q being the magnitude of the scattering vector given by $q = [4\pi n \sin(\theta/2)]/\lambda$, where n is the refractive index of the solvent, λ is the wavelength of laser light, and θ is the scattering angle) measurements were made at five different angles ranging from 50 to 130°. The change in the refractive index and the viscosity of water upon addition of salt were taken into account while analyzing the correlation function data. The apparent equivalent hydrodynamic radii of the micelles were calculated using the Stokes−Einstein relationship.

SANS measurements were carried out on the samples prepared in D_2O at the SANS facility at DHRUVA reactor, Trombay. The mean incident wavelength was 5.2 Å with $\Delta\lambda/\lambda = 15\%$. The scattering was measured in the scattering vector (q) range of 0.017−0.3 $Å^{-1}$. The measured SANS data were corrected for the background, the empty cell contributions, and transmission, and were placed on an absolute scale using standard protocols. Correction due to the instrumental smearing was taken into account throughout the data analysis.[47]

Data Analysis. The differential scattering cross-section per unit volume ($d\Sigma/d\Omega$) of monodisperse micelles can be written as[48,49]

$$d\Sigma/d\Omega = NF_{mic}(q)S(q) + B \quad (1)$$

where N is the number density of the micelles, and B is a constant term that represents the incoherent background scattering mainly from the hydrogen atoms present in the sample. $F_{mic}(q)$ is the form factor characteristic of specific size and shape of the scatterers, and $S(q)$ is the structure factor that accounts for the interparticle interaction. The block copolymer micelles can be considered as a core−shell particle with different scattering length densities of the core and the shell. The structure of these micelles is described using a model consisting of PEO chains attached to the surface of the PPO core.[48,49] The form factors for spherical and ellipsoidal micelles were used as formulated by Pedersen.[49] In this model the shell is described as consisting of noninteracting Gaussian polymer chains, and these chains are assumed to be displaced from the core (else the mathematical approximations will not work as the chains overlap each other and the core), that is, a mushroom polymer configuration is assumed. Nonpenetration of the chains into the core region is mimicked by moving the center of mass of the chains by a distance R_g away from the surface of the core, where R_g is the radius of the gyration of the chains. The form factor of the micelles $F_{mic}(q)$ comprises four terms: the self-correlation of the core, the self-correlation of the chains, the cross term between core and chains, and the cross term between different chains. The interparticle structure factor $S(q)$ for the spherical block copolymer micelles is usually captured by the analytical solution of the Ornstein−Zernike equation with the Percus−Yevick approximation, employing hard-sphere interaction.[50] The effect of intermicellar attractive interaction is generally taken into account by considering a thin adhesive surface on the hard spheres, and the effective potential is expressed in terms of Baxter potential:[51]

$$\frac{\varphi(r)}{k_BT} = \begin{cases} +\infty \text{ for } 0 < r < R' \\ \Omega \text{ for } R' < r < R \\ 0 \text{ for } R < r \end{cases}$$

and where surface potential $\Omega = \ln[12\tau(R-R'/R)]$, with $(R-R'/R)$ as the fractional surface layer thickness (ε). The structure factor for the adhesive hard sphere is thus a function of micellar volume fraction, attractive potential (Ω) or stickiness parameter ($1/\tau$), and the fractional surface layer thickness (ε), the explicit expression for which is available in the literature.[36]

In case of polydisperse micelles, eq 1 can be written as

$$d\Sigma/d\Omega = \int d\Sigma/d\Omega(q,R_c)f(R_c)dR_c + B \quad (2)$$

The polydispersity in the micellar size ($R = R_c$) has been accounted by a Schultz distribution as given by eq 3,

$$f(R_c) = [(z+1)/R_{cm}]^{z+1}R_c^z \exp[(z+1)/R_{cm}](1/(\Gamma(z+1)) \quad (3)$$

where R_{cm} is the mean value of the distribution and z is the width parameter. The polydispersity of this distribution is given by $\Delta R_c/R_{cm} = 1/(z+1)^{1/2}$.

The relative viscosity (η_r), defined as the ratio of the solution viscosity to the solvent viscosity, generally consists of contributions arising from hydrodynamic as well as interparticle interactions and can be written as[52,53]

$$\eta_r = \eta_{HD} + \eta_I \quad (4)$$

where η_{HD} is the hydrodynamic viscosity, which is calculated here using the Batchelor−Green equation, that is, $\eta_{HD} = 1 + 2.5\phi + 5.2\phi^2$, and η_I is the viscoelastic contribution arising from intermicellar interaction that is expressed in terms of the structure factor $S(Q)$:

$$\eta_I = \frac{\chi}{40\pi}\int_0^\infty dQQ^2\, d(Q)\frac{[S'(Q)]^2}{S(Q)}$$

where χ is the value of the pair correlation function at contact and $d(Q) = 1 - j_0(Q) + 2j_2(Q)$, with $j_i(x)$ being the ith-order spherical Bessel function.

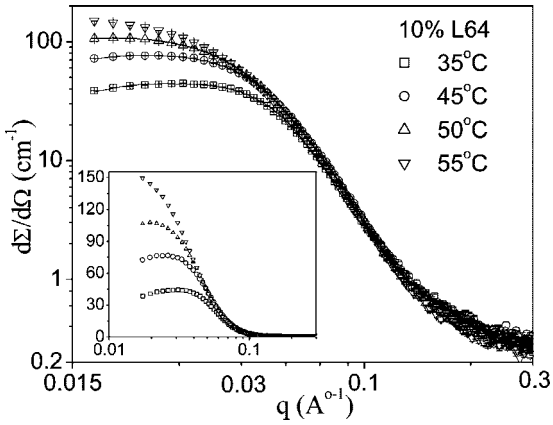

Figure 1. The SANS patterns of the 10% L64 solution at different temperatures. The solid lines represent fit to the data using ellipsoidal form factor. The inset shows the log−log plots of SANS patterns of the 1% L64 solution at 40 and 50 °C and their slopes at low q.

Results and Discussions

In view of the ambiguity over the structure of the L64 micelles, we first show (Figure 1) our SANS studies on the L64 solutions at different temperatures. Since the experimental studies on the L64 solutions report that its micelles are of spherical shape having intermicellar attractive interaction,[35−39] attempts were first made to fit the data based on spherical form factor and a structure factor comprising hard spheres with a short-range attractive potential in the form of Baxter potential. The fitted values of the parameters, however, showed unacceptably low values of micellar volume fraction (lower than the volume fraction of the copolymer) and very high values of the normalization constant (between 4−5), suggesting that this model may not be the true representation of the structure of the L64 micelles. This forced us to go by the findings of the theoretical paper[40] and to fit the data based on a ellipsoidal core-corona model with hard-sphere repulsive potential. This leads to a significantly improved fit to the data (Figure 1) with close to one-third of the χ^2 values obtained with spherical-shaped micelles and with rational values of the fitted parameters (Table 1). The results show that up to 50 °C the aggregation number of the micelles increases steadily, associated with a simultaneous increase in their aspect ratio and the cross-sectional radius. Further, the micellar volume fraction decreases with increase in temperature. This could arise due to a decrease in the solubility of the copolymer molecules and consequent decrease in the degree of micellar hydration with increase in temperature. The optimum parameters of the SANS analysis show that, despite the observed decrease in the degree of micellar hydration with increase in temperature, the hard-sphere radius increases at a faster rate than the cross-sectional radius. This could be attributed to an increase in the effective volume of the intermicellar interaction arising due to an increase in the micellar rod length upon warming. The observations of large increase in the scattering intensity and disappearance of the correlation peak at 55 °C could arise either due to the formation of micellar clusters in presence of attractive interaction or due to the large growth of the individual micelles. The quantitative estimate of the length of the micelles in this temperature range cannot be obtained from our SANS data due to the limited q-range of the SANS measurement (lowest q value of 0.015 Å^{-1}). This limits the maximum measurable micellar length to about 22 nm, which is already achieved at 50 °C (Table 1). We are thus unable to differentiate the role of micellar growth and intermicellar interaction in the observed enhancement in the viscosity near the cloud point. To understand more about the micellar structure we carried out SANS measurements on 1% L64 solutions and calculated the corresponding pair distance distribution function [$p(r)$] using the program GENOM made by Svergun and A. Semenyuk.[54,55] As shown in Figure 2, an increase in the scattering intensity with increase in temperature from 40 to 50 °C is indicative of the occurrence of micellar growth. The values of the slopes in the low q region, represented as solid lines, were found to be close to 0.5 and 1.0 at 40 and 50 °C, respectively. This suggests that these micelles are asymmetric with elliptical shape at 40 °C and become rod-like at 50 °C. The asymmetric nature of the pair distance distribution plots obtained from these plots, shown in the inset of the figure, also suggests that the micelles are anisotropic with ellipsoidal structure, the aspect ratio of which increases with increase in temperature. These SANS results thus suggest that the L64 micelles, as has been predicted by the theoretical calculations, form prolate ellipsoidal structure, the aspect ratio of which increases steadily with increase in temperature, ultimately leading to the formation of rod-like structures. In the following sections we will discuss the results of our viscosity and DLS studies and show that the observed change in the nature of the SANS spectra above 50 °C is consistent with a large increase in the size of the copolymer micelles.

To understand more about the changes in micellar characteristics with increase in temperature, the viscosity of the copolymer solutions as a function of both the temperature and the copolymer concentrations have been measured. The relative viscosity versus temperature plots for 3 and 20% copolymer concentrations are shown in Figure 3. For both solutions, it increases marginally but steadily up to 50 °C and then shows an abrupt increase above 50 °C up to the cloud point of the solution. The measurements were carried out up to 0.5 °C below the cloud point, which increases from 57.5 °C for a 3% solution to 60.5 °C for a 20% solution, similar to what is observed by Zhou and Chu.[56] The viscosity of the aqueous pluronic solutions generally decreases with increase in temperature due to decrease in the micellar hydration and a subsequent decrease in the micellar volume fraction.[57] The observed opposite behavior in the present case could be explained in terms of the previously discussed SANS results, which show that the length of the prolate-shaped L64 micelles increases slowly but steadily up to 50 °C. This probably compensates more than the decrease in viscosity expected due to a decrease in micellar volume fraction with increase in temperature. The large increase in viscosity observed above 50 °C could be attributed either to the onset of strong intermicellar attractive interaction or to an increase in the micellar length. SANS studies reported in the literature claimed that at low L64 concentration the stickiness parameter ($1/\tau$) reaches as high as 8.75 near the cloud point, close to the critical value (10.3),[37−39] considering that the relative viscosity of the 3% solutions should have reached as high as about 25 cp (calculated using eq 4 with $1/\tau = 8.75$ ($\Omega = -4.3$) and fractional surface layer thickness (ε) of 0.01), much higher than that observed experimentally near the cloud point. This suggests that the stickiness parameter of the micelles does not reach close to the critical value in this aqueous copolymer system on approaching the cloud point.

In literature, the inference about the percolation transition in the L64 solutions has been made based on viscoelastic studies on 10, 15, and 20% copolymer solutions.[37] Since no studies were carried out to understand its impact at lower copolymer concentration, we studied the concentration dependence of maximum viscosity observed near the cloud point. Figure 4

TABLE 1: Core Radius (R_c), Hard-sphere Radius (R_{hs}), Rod Length (L), Aggregation Number (N_{agg}), Volume Fraction (ϕ), and Polydispersity ($\Delta R_c/R_{cm}$) of the Micelles in 10% Block Copolymer $(EO)_{13}(PO)_{30}(EO)_{13}$ Solutions and the Reduced χ^2 Values of the Fits at Different Temperatures[a]

T (°C)	R_c (nm)	L (nm)	N_{agg}	R_{hs} (nm)	ϕ	$\Delta R_c/R_{cm}$ (%)	χ^2
35 °C	2.39 ± 0.01	10.2 ± 0.4	88	5.79 ± 0.03	0.152 ± 0.004	25.6 ± 0.3	2.2
45 °C	2.77 ± 0.01	15.3 ± 0.2	170	6.65 ± 0.04	0.138 ± 0.004	20.5 ± 0.2	1.9
50 °C	2.885 ± 0.005	22.7 ± 0.2	275	7.74 ± 0.03	0.116 ± 0.002	22.2 ± 0.5	2.9
30 °C	1.94 ± 0.01	08.9 ± 0.3	49	5.78 ± 0.05	0.106 ± 0.003	33.6 ± 0.5	3.9
30 °C, 1 M NaCl	2.81 ± 0.05	17.4 ± 0.4	200	6.63 ± 0.04	0.150 ± 0.005	22.9 ± 0.4	3.1

[a] The R_g values remains in the range 0.6 ± 0.1 nm. Aggregation number has been calculated from the total core volume of the micelles divided by the volume of PPO block.

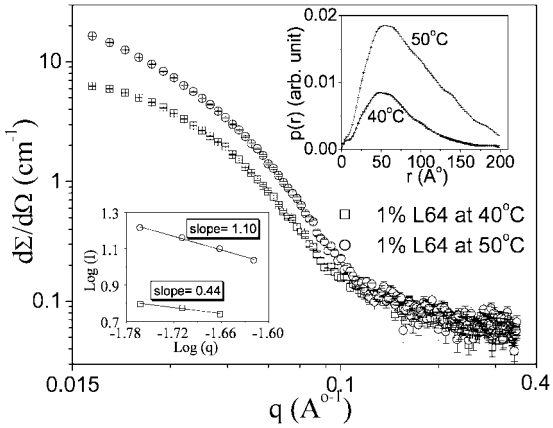

Figure 2. The SANS patterns of the 1% L64 solution at different temperatures. The insets show the corresponding pair distance distribution function [$p(r)$] plots and the slopes of the log(I) vs log(q) plots in the low q region.

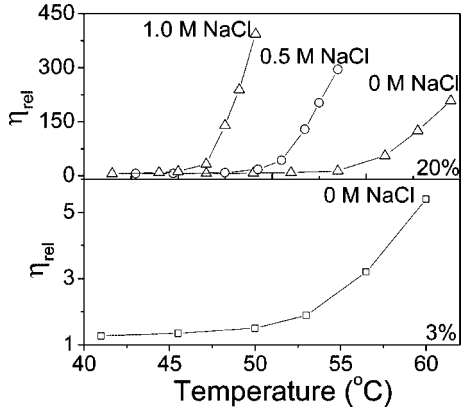

Figure 3. Relative viscosity (η_{rel}) vs temperature plots for 20 and 3% L64 solutions.

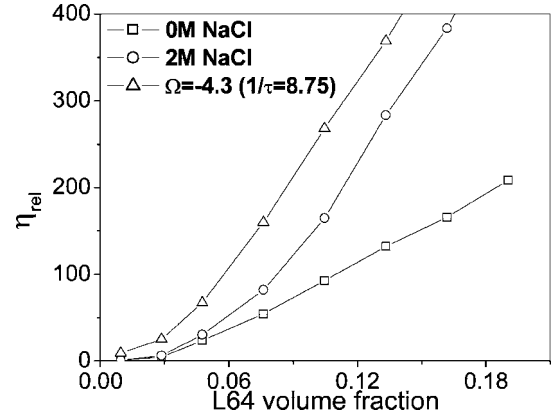

Figure 4. Relative viscosity (η_{rel}) vs L64 concentration plots in the presence and the absence of 2 M NaCl. The calculated plot is generated based on eq 4, with the fractional surface layer thickness (ε) of 0.01.

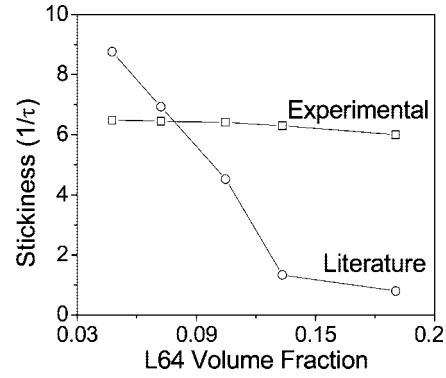

Figure 5. Stickiness parameter values ($1/\tau$) calculated from the viscosity plot shown in Figure 3 and their approximate values obtained from ref 34. The calculations were done based on eq 4, with the fractional surface layer thickness (ε) of 0.01.

shows a comparison of the experimentally observed variation in the viscosity with L64 volume fraction with that generated with eq 4 for stickiness parameter ($1/\tau$) values of 8.75 ($\Omega = -4.3$). The copolymer volume fractions were calculated from the density of the L64 (1.05 g/cc), as mentioned in the BASF technical report. Since our SANS results show that near the cloud point the micellar volume fraction reaches close to its limiting value of the copolymer volume fraction due to progressive decrease in the micellar degree of hydration, the viscosity values were plotted against the copolymer volume fraction used. Figure 4 shows that in the entire copolymer concentration range investigated the calculated viscosities are significantly higher than the experimentally observed values. This suggests that the attractive potential remains much lower than the critical value at all measured concentrations. Previous reports based on SANS analysis show that near the cloud point the stickiness parameter ($1/\tau$) reaches as high as 8.8 for 5% copolymer concentration and that it decreases significantly with increase in the copolymer concentrations.[38,39] In Figure 5 we have compared these reported values of the stickiness parameter with those calculated by us from the viscosity plot (Figure 4) using eq 4. The figure shows that, in the entire copolymer concentration range studied, the stickiness parameter plot corresponding to the observed viscosity values is different from those reported from the SANS analysis.[38,39] At low copolymer concentration, the stickiness parameters obtained by us are significantly lower than those reported from the SANS analysis, and the observed viscosities of the copolymer solutions are also not as high as to match the predicted percolation.[38,39] At higher copolymer concentration the reported values of the stickiness parameter are much lower than those obtained by us from the viscosity measurements due to a sharp drop in the turbidity of the copolymer solutions with increase in the copolymer con-

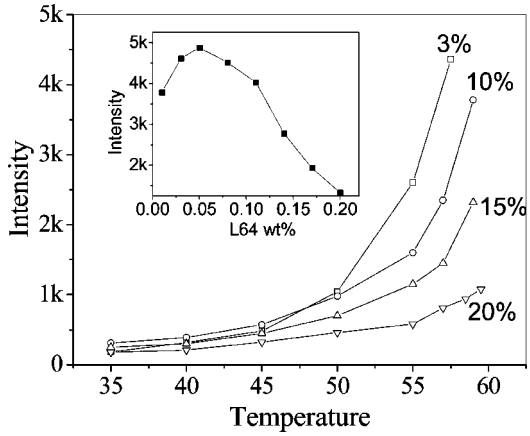

Figure 6. Scattered light intensity vs temperature plots for different L64 concentrations. Inset shows the variation of the maximum scattering intensity observed vs L64 concentration.

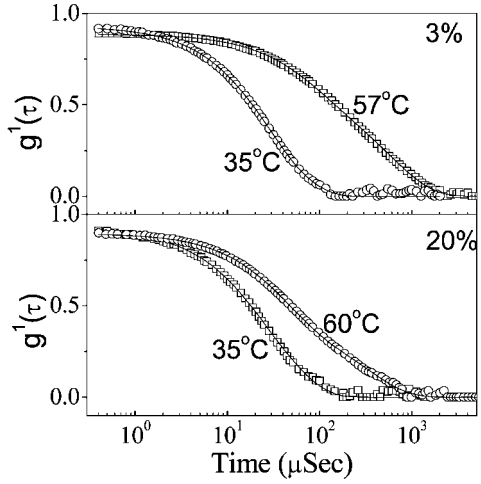

Figure 7. Correlation function diagram vs time plots for 3 and 20% L64 solutions at 35 °C and near the cloud point. The solid lines represent fit to the data.

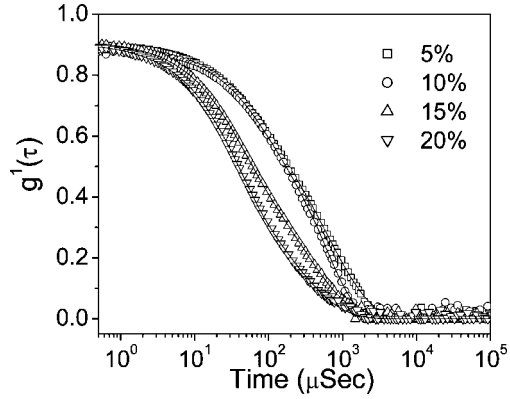

Figure 8. Variation of the correlation function diagram vs time plots with L64 concentration near the cloud point. The solid lines represent fit to the data.

centration. The incompatibility of the stickiness parameter values obtained from the viscosity and the SANS measurements shows that the adhesive hard-sphere model used to explain the observed turbidity of the L64 solutions near the cloud point fails to shed light on their viscosity behavior. The values of the stickiness parameter obtained from the viscosity plot are not their true values and only represent the enhanced viscosity of the copolymer solutions near the cloud point, presumably due to a sphere-to-rod micellar shape transition. To throw further light on this system we will now discuss our DLS studies on it. The high viscosity of the copolymer solutions in this copolymer concentration range could arise due to the formation of worm-like micelles.

TABLE 2: The Amplitude (A_s), Relaxation Time (τ_s), and the Stretching Exponent (β) for the Slow Relaxation Mode As a Function of Copolymer Concentration

copolymer conc. (%)	A_s	τ_s (μs)	β
3	0.76	429.2	0.75
5	0.75	571.4	0.73
8	0.77	909.1	0.72
11	0.71	606.1	0.71
14	0.70	354.6	0.69
17	0.63	243.3	0.68
20	0.55	196.1	0.66

The variation in scattering intensity with temperature for 3, 10, 15, and 20% L64 solutions on approaching their cloud points (up to 0.5 °C below CP) are shown in Figure 6. At all concentrations, the scattering intensity initially increases slowly with increase in temperature and then more rapidly above 50 °C. The variation in the maximum intensity attained near the respective cloud points with L64 concentrations is shown as an inset of Figure 6. The scattering intensity increases initially up to 5% and then decreases with increase in the L64 concentration; the decrease from 10 to 15% is more notable. The observation of high scattering intensity in the solutions containing low L64 concentrations near the cloud point has been explained in the literature based on critical concentration fluctuation.[35−39,58−63] It has been argued that a divergence in the mass of the micellar aggregates on approaching the cloud point due to the development of an intermicellar attractive interaction is responsible for this observation. They have shown that although at low copolymer concentration the stickiness parameter of the micelles reaches close to the critical value ($1/\tau = 10.3$), it remains much smaller near the cloud point at higher copolymer concentration ($\leq$15%).[35−39] Figure 6 shows that although 3, 10, and 15 L64 solutions show a significant increase in the scattering intensity near the cloud point, the same is not true for the 20% solution. This solution does not develop any visible turbidity in it until it phase separates at the cloud point. This also suggests that at high copolymer concentration the attractive interaction weakens and thus significant numbers of micellar clusters are not formed on approaching the cloud point. In view of this, the observed increase in viscosity in this system near cloud point can be best explained in terms of the anisotropic growth of the micellar structures.

Figure 7 shows the variation in the intensity correlation function of 3 and 20% L64 solutions at different temperatures. The observed increase in the scattering intensity near the cloud point is coincident with a shift in the correlation function versus time plots to longer time scale, indicating the occurrence of micellar growth in that temperature range. To compensate for the change in the viscosity of water with increase in temperature, the correlation function near the cloud points were normalized with respect to 35 °C based on the following equation:[64]

$$t_{\text{norm}} = t\frac{T}{308}\frac{\eta_{308}}{\eta_T} \tag{6}$$

For both concentrations, the decay of the correlation function undergoes changes with increase in temperature from single

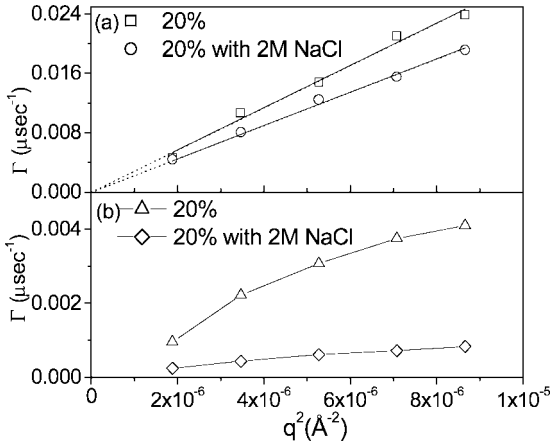

Figure 9. Γ vs q^2 plots of the faster and slower mode in the 20% L64 solutions.

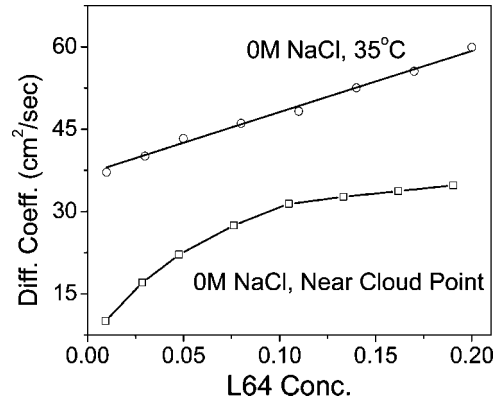

Figure 10. Diffusion coefficient vs copolymer concentration plots of the L64 micelles at 35 °C and near the cloud point.

exponential to double exponential. This signifies the presence of a slower-moving species near the cloud point along with the micelles. The observed changes in the correlation function as a function of copolymer concentration near the cloud points of the copolymer solutions is depicted in Figure 8. The change in the nature of the plot is more prominent above 10% copolymer concentration, where the observed maximum scattering intensity starts decreasing significantly. The presence of the slower mode near the cloud point could arise due to the combined effect of the presence of micellar clusters and the entanglement of the rod-like micelles. At low copolymer concentration with large critical fluctuation, the presence of micellar clusters should play a dominant role. On the other hand, at high copolymer concentrations (above 15%), where critical fluctuation does not seem to play any significant role, the observed results look similar to the entangled worm-like micellar systems.[54−59]

The analysis of these correlation functions shows that they can be best described as a sum of a single exponential and a stretched biexponential function:

$$g^{(1)}(t) = A_f \exp(-t/\tau_f) + A_s \exp[-(t/\tau_s)^{\beta}] \qquad (7)$$

where A_f and A_s are the amplitudes for the fast and slow relaxation modes corresponding to the relaxation time τ_f and τ_s, respectively, and β is the stretching exponent.[64−69] The value of these parameters for different L64 concentrations are shown in Table 2. The relaxation time for the fast mode is associated with the diffusion of the micelles, and that of the slow mode can be ascribed to the presence of micellar clusters and the coupling between concentration fluctuation or stress relaxation in entangled rod-like micelles. According to the coupling theory, the exponent β ($0 < \beta \leq 1$) is inversely proportional to the width of the distribution of the relaxation times of the slow mode, and an increase in the micellar entanglement will lead to the observation of an increase in τ_s and a decrease in β.[64−69] Coupling theory suggests that τ_f is proportional to q^{-2} and that τ_s is proportional to $q^{-2/\beta}$, and our analysis of the data shows that although the decay rates of the fast mode vary linearly with q^{-2} that of the slower mode does not show any linear variation either with $q^{-2/\beta}$ or with q^{-2} (Figure 9). A combined contribution of micellar clusters and micellar entanglement to the slow mode could be responsible for this behavior. The change in the character of the slow mode with increase in the copolymer concentration is evident from the change in the values of A_s, τ_s, and β, shown in Table 2. Significantly lower values of A_s and τ_s at 20% solution as compared to those at lower copolymer concentrations show that the size and amount clusters are significantly smaller at copolymer concentrations. This, coupled with higher polydispersity of the slow mode (lower β), and the absence of any visible turbidity in the 20% solution on approaching the cloud point suggest that the micellar entanglement is the principal contributor to the slow mode at high copolymer concentration.

Figure 10 depicts the variation of the diffusion coefficient of the micelles, as obtained from τ_f at 35 °C and near the cloud point as a function of the copolymer concentration. The figure shows that both at low and the high temperature the diffusion coefficient increases with increase in the copolymer concentrations, which suggests that the intermicellar interaction remains predominantly repulsive even near the cloud point.[70,71] The diffusion coefficient obtained near the cloud point are much lower than those obtained at 35 °C due to the growth of the micelles with increase in temperature. Because the reported stickiness parameters of the micelles are quite low at high copolymer concentrations (Figure 5), the large difference in the diffusion coefficient in that concentration range cannot be explained based on the adhesive hard-sphere model. These results thus suggest that near the cloud point the interaction between the micelles remains predominantly repulsive in nature.

We will now correlate these DLS results with the observed concentration and temperature dependence of the viscosity data discussed earlier. At low copolymer concentration, although the DLS data shows the presence of large micellar clusters and the copolymer solutions show an increase in viscosity near the cloud point, there is no sign of any percolation in the copolymer solutions. Corti and Degiorgio[72] and Zulauf and Rosenbusch[73] observed similar behavior in different oxyethylene-based nonionic micellar systems and explained them based on the formation of large but loosely bound statistical clusters due to the presence of weak intermicellar attractive interaction. These clusters, which include both micelles and water, are formed when micelles are correlated over a distance much larger than the micellar size, and can be probed by DLS along with the individual micelles.[72,73] The presence of a weak intermicellar attractive interaction has been proposed because of the fact that the presence of a strong attractive interaction would result in the observation of percolation due to the formation of stable and compact clusters, instead of loosely bound ones. In the present case, the analysis of the correlation function data shows that, apart from the appearance of slow moving species, there is significant growth of the faster-moving micelles as the temperature approaches the cloud point (Figure 10). The observed growth of the micelles and the absence of any visible turbidity

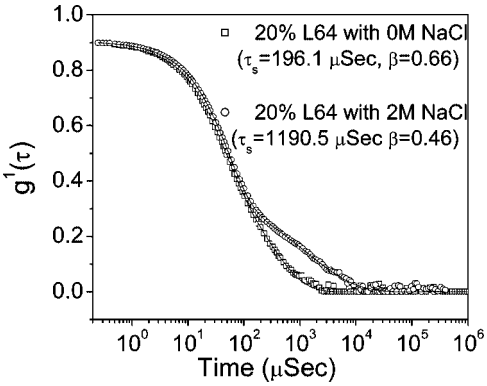

Figure 11. Correlation function diagram vs time plots for the 20% L64 solutions near the cloud point in the absence and the presence of 2 M NaCl. The solid lines represent fit to the data.

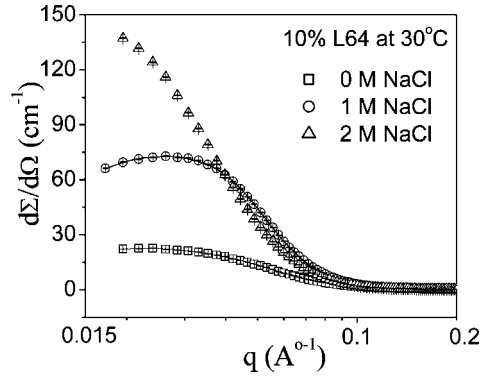

Figure 12. The SANS patterns of the 10% L64 solution with different NaCl concentrations recorded at 30 °C. The solid lines represent fit to the data using ellipsoidal form factor.

in the solutions with high copolymer concentrations suggest that the anisotropic growth of the micelles, rather than the critical concentration fluctuation, plays a dominant role in enhancing the viscosity of the copolymer solutions on approaching the cloud point. These results are consistent with those observed in other nonionic micellar systems.[74]

The Effect of NaCl. To understand the effect of the water-structure-making salts on the micellar growth behavior, we studied the effect of NaCl on the observed growth of the L64 micelles near the cloud point. NaCl is known to increase the hydrophobic character of the copolymer molecules and reduce CMC, CMT, sphere-to-rod shape transition temperature, and the cloud point. The viscosity versus temperature plots of 20% copolymer solution shown in Figure 3 at different NaCl concentration suggests that it not only lowers the micellar growth temperature but also leads to a significant increase in the maximum viscosity attained on approaching the cloud point. This is also clear from Figure 4, where the viscosity of the copolymer solutions containing 2 M NaCl measured at 0.5 °C below the cloud points is compared with those of the pure ones. The salt-containing solutions show significantly higher viscosity, and the difference in the viscosity values widens with increase in the copolymer concentrations.

Dynamic light scattering measurements were also performed on the 20% copolymer solution near the cloud point in the absence and in the presence of 2 M NaCl (Figure 11). Although the plots for both the solutions show signatures characteristics of entangled micellar systems, the larger value of τ_s and a smaller value of β in the solution containing 2 M NaCl indicate that the micellar entanglement is enhanced in the presence of NaCl. This is consistent with the observed higher value of viscosity of the NaCl-containing solutions shown in Figure 4 and could be attributed to poorer solvent quality of water in the presence of NaCl.[68] The variation of the SANS plot with NaCl concentration, shown in Figure 12, is similar to that observed with increase in temperature. The structural parameters of the micelles obtained for 1 M NaCl (Table 1) shows that micellar aggregation number and the aspect ratio increase significantly in the presence of NaCl. The plot for the 2 M NaCl-containing solution is very similar to the plot obtained for the pure L64 solution at 55 °C (Figure 1). The observed increase in the micellar volume fraction upon addition of 1 M NaCl results due to the conversion of copolymer unimers present at 30 °C into micelles.[22] These results suggest that the addition of water-structure-making salts such as NaCl can reduce the micellar growth temperature and induce formation of room-temperature worm-like micelles in the L64 solutions.

Conclusions

The interplay of growth and intermicellar interaction has been investigated in the aqueous L64 solutions near their cloud points by SANS, DLS, and viscometry measurements. The observation of critical concentration fluctuation and a concomitant enhancement in viscosity of the L64 solutions on approaching their cloud point have been explained by the previous studies based on the onset of a strong intermicellar attractive interaction. Our studies suggest that an intermicellar attractive interaction does lead to the formation of micellar clusters and consequent critical concentration fluctuation, but it does not play any significant role in observed enhancement in viscosity of the L64 solutions on approaching the cloud points. It has been shown that L64 micelles have a prolate ellipsoidal structure, and a progressive increase in their anisotropy with increase in temperature leads to an increase in viscosity of the copolymer solutions near their cloud point. It is also observed that the water-structure-making salts such as NaCl reduces the micellar growth temperature and induces the formation of worm-like micellar structures at room temperature and below.

References and Notes

(1) Chu, B. *Langmuir* **1995**, *11*, 414.
(2) Wanka, G.; Hoffmann, H.; Ulbricht, W. *Macromolecules* **1994**, *27*, 4145.
(3) Hurter, P. N.; Hatton, T. A. *Langmuir* **1992**, *8*, 1291.
(4) Schmolka, I. R. *J. Am. Oil Chem. Soc.* **1977**, *54*, 110.
(5) Pandit, N. K.; Wang, D. *Int. J. Pharm.* **1998**, *167*, 183.
(6) Zhang, K.; Khan, A. *Macromolecules* **1995**, *28*, 3807.
(7) Wanka, G.; Hoffmann, H.; Ulbricht, W. *Colloid Polym. Sci.* **1990**, *268*, 101.
(8) Hvidt, S.; Jorgensen, E. B.; Brown, W.; Schillen, K. *J. Phys. Chem.* **1994**, *98*, 12320.
(9) Alexandridis, P.; Holzwarth, J. F.; Hatton, T. A. *Macromolecules* **1994**, *27*, 2414.
(10) Mortensen, K.; Brown, W.; Norden, B. *Phys. Rev. Lett.* **1992**, *68*, 2340.
(11) Brown, W.; Schillen, K.; Almgren, M.; Hvidt, S.; Bahadur, P. *J. Phys. Chem.* **1991**, *95*, 1850.
(12) Malmsten, M.; Lindman, B. *Macromolecules* **1992**, *25*, 1282.
(13) Mortensen, K.; Pedersen, J. S. *Macromolecules* **1993**, *26*, 805.
(14) Norman, A. I.; Ho, D. L.; Karim, A.; Amis, E. J. *J. Colloid Interface. Sci.* **2005**, *288*, 155.
(15) Hamley, I. W.; Pedersen, J. S.; Booth, C.; Nace, V. M. *Langmuir* **2001**, *17*, 6386.
(16) Fairclough, J. P. A.; Norman, A. I.; Shaw, B.; Nace, V. M.; Heenan, R. K. *Polym. Int.* **2006**, *55*, 793.
(17) Castelletto, V.; Hamley, I. W. *Polymers Adv. Technol.* **2006**, *17*, 137.
(18) Castelletto, V.; Parras, P.; Hamley, I. W.; Bäverbäck, P.; Pedersen, J. S.; Panine, P. *Langmuir* **2007**, *23*, 6896.
(19) Zhou, Z.; Chu, B. *J. Colloid Interface. Sci.* **1988**, *126*, 171.
(20) Jorgensen, E. B.; Hvidt, S.; Brown, W.; Schillen, K. *Macromolecules* **1997**, *30*, 2355.

(21) Mortensen, K.; Brown, W. *Macromolecules* **1993**, *26*, 4128.
(22) Al-saden, A. A.; Whateley, T. L.; Florence, A. T. *J. Colloid Interface. Sci.* **1982**, *90*, 303.
(23) Schillen, K.; Brown, W.; Johnson, R. M. *Macromolecules* **1993**, *27*, 4825.
(24) 2leischer, G. *J. Phys. Chem.* **1993**, *97*, 517.
(25) Glatter, O.; Scherf, G.; Schillen, K.; Brown, W. *Macromolecules* **1994**, *27*, 6046.
(26) Lehner, O.; Lindner, H.; Glatter, O. *Langmuir* **2000**, *16*, 1689.
(27) Lindner, H.; Scherf, G.; Glatter, O. *Phys. Rev. E* **2003**, *67*, 061402.
(28) Waton, G.; Michels, B.; Steyer, A.; Schosseler, F. *Macromolecues* **2004**, *37*, 2313.
(29) Duval, M.; Waton, G.; Schosseler, F. *Langmuir* **2005**, *21*, 4904.
(30) King, S. M.; Heenan, R. K.; Cloke, V. M.; Washington, C. *Macromolecues* **1997**, *30*, 6225.
(31) Michels, B.; Waton, G.; Zana, R. *Colloids Surf., A* **2001**, *183*−*185*, 55.
(32) Ganguly, R.; Aswal, V. K.; Hassan, P. A.; Gopalakrishnan, I. K.; Yakhmi, J. V. *J. Phys. Chem. B* **2005**, *109*, 5653.
(33) Bahadur, P.; Pandya, K.; Almgren, M.; Li, P.; Stilbs, P. *Colloid Polym. Sci.* **1993**, *271*, 657.
(34) Linse, P. *J. Phys. Chem.* **1993**, *97*, 13896.
(35) Chen, W.-R.; Mallamace, F.; Glinka, C. J.; Fratini, E.; Chen, S.-H. *Phys. Rev. E* **2003**, *68*, 041402.
(36) Liu, Y. C.; Chen, S.-H.; Huang, J. S. *Phys. Rev. E* **1996**, *54*, 1698.
(37) Lobry, L.; Micali, N.; Mallamace, F.; Liao, C.; Chen, S.-H. *Phys. Rev. E* **1999**, *60*, 7076.
(38) Liao, C.; Choi, S.-M.; Mallamace, F.; Chen, S.-H. J. *Appl. Cryst.* **2000**, *33*, 677.
(39) Chen, S.-H.; Liao, C.; Fratini, E.; Baglioni, P.; Mallamace, F. *Colloids Surf., A* **2001**, *183*−*185*, 95.
(40) Bedrov, D.; Smith, G. D.; Yoon, J. *Langmuir* **2007**, *23*, 12032.
(41) Israelachvili, J. N.; Mitchell, D. J.; Ninham, B. W. *J. Chem. Soc., Faraday Trans. 2* **1976**, *72*, 1525.
(42) Bossev, D. P.; Kline, S. R.; Israelachvili, J. N.; Paulaitis, M. E. *Langmuir* **2001**, *17*, 7728.
(43) *ASTM Standard D 445*−*04 and D 446*−*04*, **2004**, and references therein.
(44) Hassan, P. A.; Kulshreshtha, S. K. *J. Colloid Int. Sc.* **2006**, *300*, 744.
(45) Koppel, D. E. *J. Chem. Phys.* **1972**, *57*, 4814.
(46) Pecora, R. *Dynamic Light Scattering: Application of Photon Correlation Spectroscopy*; Plenum Press: New York, 1985.
(47) Aswal, V. K.; Goyal, P. S. *Curr. Sci.* **2000**, *79*, 947.
(48) Pedersen, J. S.; Gerstenberg, C. *Macromolecules* **1996**, *29*, 1363.
(49) Pedersen, J. S. *J. Appl. Crystallogr.* **2000**, *33*, 637.
(50) Percus, J. K.; Yevick, G. J. *Phys. Rev.* **1958**, *1*, 110.
(51) (a) Baxter, R. J. *J. Chem. Phys.* **1968**, *49*, 2770. (b) **1970**, *52*, 4559.
(52) De Schepper, I. M.; Smorenburg, H. E.; Cohen, E. G. D. *Phys. Lett.* **1993**, *5*, 2178.
(53) Liu, Y. C.; Sheu, E. Y. *Phys. Rev. Lett.* **1996**, *76*, 700.
(54) Svergun, D. I.; Semenyuk, A. V.; Feigin, L. A. *Acta Cryst. A* **1988**, *44*, 244.
(55) Svergun, D. I. *J. Appl. Crystallogr.* **1991**, *24*, 485.
(56) Zhou, Z.; Chu, B. *Macromolecules* **1994**, *27*, 2025.
(57) Bahadur, P.; Pandya, K. *Langmuir* **1992**, *8*, 2666.
(58) Kositza, M. J.; Bohne, C.; Alexandridis, P.; Hatton, T. A.; Holzwarth, J. F. *Langmuir* **1999**, *15*, 322.
(59) Almgren, M.; Bahadur, P.; Jansson, M.; Li, P.; Brown, W.; Bahadur, A. *J. Colloid Interface Sci.* **1992**, *151*, 157.
(60) Al-Saden, A. A.; Whateley, T. L.; Florence, A. T. *J. Colloid Interface Sci.* **1982**, *90*, 303.
(61) Zhou, D.; Alexandridis, P.; Khan, A. *J. Colloid Interface Sci.* **1996**, *183*, 339.
(62) Yang, L.; Alexandridis, P.; Steytler, D. C.; Kositza, M. J.; Holzwarth, J. F. *Langmuir* **2000**, *16*, 8555.
(63) Pandya, K.; Bahadur, P.; Nagar, T. N.; Bahadur, A. *Colloids Surf., A* **1993**, *70*, 219.
(64) Moitzi, C.; Freiberger, N.; Glatter, O. *J. Phys. Chem. B* **2005**, *109*, 16161.
(65) Adam, M.; Delsanti, M. *Macromolecules* **1985**, *18*, 1760.
(66) Nystrom, B.; Thuresson, K.; Lindman, B. *Langmuir* **1995**, *11*, 1994.
(67) Sun, Z.; Wang, C. H. *Macromolecules* **1994**, *27*, 5667.
(68) Ngai, K. L. *Adv. Colloid Interface Sci.* **1996**, *64*, 1.
(69) Ganguly, R.; Aswal, V. K.; Hassan, P. A. *J. Colloid Interface Sci.* **2007**, *315*, 693.
(70) Kato, T.; Seimiya, T. *J. Phys. Chem.* **1986**, *90*, 3159.
(71) Ishikawa, M.; Matsumura, K.-I.; Esumi, K.; Meguro, K.; Limbele, B.; Zana, R. *J. Colloid Interface Sci.* **1992**, *151*, 70.
(72) Corti, M.; Degiorgio, V. *J. Phys. Chem.* **1981**, *85*, 1442.
(73) Zulauf, M.; Rosenbusch, J. P. *J. Phys. Chem.* **1983**, *87*, 856.
(74) Glatter, O.; Fritz, G.; Lindner, H.; Brunner-Popela, J.; Mittelbach, R.; Strey, R.; Egelhaaf, S. U. *Langmuir* **2000**, *16*, 8692.

JP808304W